

UNIVERSIDAD DE LOS ANDES



# Phenomenological Study of Search of Heavy Neutrinos, with Displaced Vertices and Vector Boson Fusion

THIS DISSERTATION IS SUBMITTED FOR THE DEGREE OF

PHYSICIST

BY

SANDRA JIMENA GONZÁLEZ LOZANO

ADVISOR: ANDRÉS FLÓREZ

BOGOTÁ, D.C.

2017

# Contents

<b>1</b>	<b>State of the Art</b>	<b>1</b>
1.1	Standard Model . . . . .	1
1.1.1	Higgs Mechanism . . . . .	1
1.2	Neutrinos in the Standard Model . . . . .	1
1.2.1	Dirac Mass . . . . .	1
1.2.2	Majorana Mass . . . . .	2
1.3	Seesaw Mechanism . . . . .	4
<b>2</b>	<b>CMS Detector</b>	<b>7</b>
2.1	Accelerator and Storage Ring . . . . .	8
2.2	Tracks Detector . . . . .	8
2.3	Calorimetry . . . . .	9
2.3.1	Electromagnetic Calorimeter . . . . .	9
2.3.2	Hadronic Calorimeter . . . . .	10
2.4	Muon Detector . . . . .	10
2.5	Triggers . . . . .	10
2.5.1	Triggers at the CMS . . . . .	10
<b>3</b>	<b>Important Concepts and Variable Definitions</b>	<b>11</b>
3.1	Jets . . . . .	11
3.2	Cross Section and Luminosity . . . . .	12
3.3	Pseudorapidity . . . . .	13
3.4	$p_T$ and $E_T^{\vec{miss}}$ . . . . .	14
3.5	Displaced Vertices and Impact Parameter . . . . .	14

<i>CONTENTS</i>	2
<b>4 Model and backgrounds</b>	<b>17</b>
4.1 Signal of Interest . . . . .	17
4.2 Backgrounds . . . . .	17
4.2.1 W + Jets Background . . . . .	17
4.2.2 Drell Yan + Jets Background . . . . .	17
4.2.3 $t\bar{t}$ Background . . . . .	17
<b>5 Methodology</b>	<b>18</b>
5.1 MadGraph . . . . .	18
5.2 Pythia . . . . .	18
5.3 Delphes . . . . .	18
5.4 ROOT . . . . .	18
<b>6 Analysis</b>	<b>19</b>
<b>7 Event Selection Criteria</b>	<b>20</b>
<b>8 Conclusions</b>	<b>21</b>
<b>Appendix A Neutrinos and Seesaw Mechanism</b>	<b>22</b>
A.0.1 Dirac Mass . . . . .	22
A.0.2 Majorana Mass . . . . .	23
<b>Appendix B Charge Conjugation Operator</b>	<b>26</b>

# Chapter 1

## State of the Art

### 1.1 Standard Model

#### 1.1.1 Higgs Mechanism

### 1.2 Neutrinos in the Standard Model

As it was mentioned earlier, the SM does not explain the reason why the mass of neutrinos is a factor of almost  $10^{-6}$  smaller than the mass of the other fermions. Moreover the SM predicts that the mass of the neutrinos is zero. Additionally, it does not provide an explanation to the fact that only left-handed neutrinos have been observed in nature. In this section we are going to work on possible solutions to these problems. <sup>1</sup>

#### 1.2.1 Dirac Mass

First, we start by studying the Dirac mass term of a free fermion. The Lagrangian equation for a fermion particle is given by the expression:

$$L = \bar{\psi} (i\gamma^\mu \partial_\mu - m) \psi \quad (1.1)$$

Where  $\psi$  is the Dirac Spinor. From this Lagrangian expression it is possible to see that in the SM the mass is included through the second term in the equation which is called “Dirac mass term”:

---

<sup>1</sup>The detailed calculations of the theory explained here are stated in A

$$m\bar{\psi}\psi \quad (1.2)$$

We can write the Dirac Spinor as a sum of its left- and right- chiral states:

$$m\bar{\psi}\psi = m(\bar{\psi}_L + \bar{\psi}_R)(\psi_L + \psi_R) = m\bar{\psi}_L\psi_R + m\bar{\psi}_R\psi_L \quad (1.3)$$

Previously we have used the fact that:  $\bar{\psi}_L\psi_L = \bar{\psi}_R\psi_R = 0$  which is proved in Appedix A. It can be seen from the lastest equation that a massive particle must have both quiral states: left and right. Thus, the Dirac Mass can be interpreted as the coupling constant between the two chiral states. Since right-handed neutrinos had been never observed in nature, it is expected that neutrinos have zero mass. Although, experiments of neutrino oscillations indicate that neutrinos have a small mass of the order of meV. The former implies either the existence of a right-handed neutrino which is responsible for the mass of the neutrino, or that there exists other sort of mass term.

### 1.2.2 Majorana Mass

The Majorana Mechanism is based on expressing the mass term in the Lagrangian in only the left-handed chiral state terms. To do this we start by decomposing the wavefunction into its left and right chiral states in the Dirac Lagrangian:

$$\begin{aligned} L &= \bar{\psi}(i\gamma^\mu\partial_\mu - m)\psi \\ &= (\bar{\psi}_L + \bar{\psi}_R)(i\gamma^\mu\partial_\mu - m)(\psi_L + \psi_R) \\ &= i\bar{\psi}_L\gamma^\mu\partial_\mu\psi_L - \bar{\psi}_Lm\psi_R + i\bar{\psi}_R\gamma^\mu\partial_\mu\psi_R - \bar{\psi}_Rm\psi_L \end{aligned} \quad (1.4)$$

Since  $\bar{\psi}_L\psi_L = \bar{\psi}_R\psi_R = 0$  and  $\bar{\psi}_R\gamma^\mu\partial_\mu\psi_L = \bar{\psi}_L\gamma^\mu\partial_\mu\psi_R = 0$  as it is explained in the Appendix A. Now, we can replace the expression of this Lagrangian in the Euler-Lagrange equation:

$$\frac{\partial L}{\partial(\partial\phi)} - \frac{\partial L}{\partial\phi} = 0 \quad (1.5)$$

By doing this we find that the two equations of motion for the fields are two coupled Dirac equations for the right- and left- handed fields:

$$i\gamma^\mu \partial_\mu \psi_L = m\psi_R \quad (1.6)$$

$$i\gamma^\mu \partial_\mu \psi_R = m\psi_L \quad (1.7)$$

In the formulation of the SM the mass of the neutrino is zero, in this case we obtain two equations which are called “Weyl equations”:

$$i\gamma^\mu \partial_\mu \psi_L = 0 \quad (1.8)$$

$$i\gamma^\mu \partial_\mu \psi_R = 0 \quad (1.9)$$

The former means that neutrinos can be described using two two-component spinors that are helicity eigenstates. These eigenstates represent two states with definite and opposite helicity which correspond to the left- and right-handed neutrinos. However, since we have not observed a right-handed neutrino we just represent the neutrino as a single left-handed massless field.

Majorana worked out a way to describe a massive neutrino just in terms of it's left-handed field. This calculation is performed in the Appendix A. The objective of Majorana was to write the Equation 1.7 as 1.6 by finding an expression for  $\psi_R$  in terms of  $\psi_L$ . By doing some manipulations of the Equation 1.7 we find that it can be written as:

$$i\gamma^\mu \partial_\mu C\bar{\psi}_R^\top = mC\bar{\psi}_L^\top \quad (1.10)$$

Where  $C$  is the operator charge conjugation operator. This operator and its properties are explained in Appendix B. Now, the Equation 1.10 would have the same structure as Equation 1.6 if the right-handed term is imposed to be:

$$\psi_R = C\bar{\psi}_L^\top \quad (1.11)$$

The former assumption requires  $C\bar{\psi}_L^\top$  to be right-handed, this is proved in the Appendix A. Thus, the complete Majorana field can be written as:

$$\psi = \psi_L + \psi_R = \psi_L + C\bar{\psi}_L^\top \quad (1.12)$$

Defining the charge-conjugate field as:  $\psi_L^C = C\overline{\psi}_L^T$ . We get for the expression of the complete Majorana field:

$$\psi = \psi_L + \psi_L^C \quad (1.13)$$

The implications of requiring the right-handed component of  $\psi$  to satisfy the 1.13 expression can be studied by taking the charge conjugate of the complete Majorana field.

$$\psi^C = (\psi_L + \psi_L^C)^C = \psi_L^C + \psi_L = \psi \quad (1.14)$$

Having in mind that the charge conjugation operator turns a particle state into an antiparticle state, it can be deduced that a Majorana particle is its own antiparticle. Since the charge conjugation operator flips the sign of electric charge, a Majorana particle must be neutral. Thus, the neutrino is the only fermion that could be a Majorana particle.

### Majorana Mass Term

Previously, we saw that the mass term in the Lagrangian couples the left and right chiral states of the neutrino (Equation 1.3). Replacing the expression we found for the right-handed component of the neutrino field in the mass term of the Lagrangian, we get (having in mind that its hermitian conjugate is identical):

$$L_{Maj}^L = m\overline{\nu}_L\nu_L^C + m\nu_L^C\overline{\nu}_L = \frac{1}{2}m\nu_L^C\overline{\nu}_L \quad (1.15)$$

## 1.3 Seesaw Mechanism

As it was mentioned before, in the case that the right-handed chiral field does not exist there can be no Dirac mass term. However we can have a Majorana mass term in the Lagrangian so the neutrino would be a Majorana particle:

$$L_{Maj}^L = \frac{1}{2}m_L\nu_L^C\overline{\nu}_L \quad (1.16)$$

The term  $m_L$  is forbidden by electroweak symmetry and it appears after its spontaneous breakdown through the Higgs Mechanism, hence

such a term can not exist. In order to let the neutrino to have mass, a right-handed neutrino that interacts only with gravity and the Higgs mechanism must exist. If we consider that a right-handed chiral neutrino can exist, we would have to add different terms to the Lagrangian. First, if we assume that it is possible to write a left-handed Majorana field, we have for the first term:

$$L_L^M = m_L \bar{\nu}_L^C \nu_L + m_L \bar{\nu}_L^C \nu_L \quad (1.17)$$

Additionally, we have to include a similar term which is the right-handed Majorana field:

$$L_R^M = m_R \bar{\nu}_R^C \nu_R + m_R \bar{\nu}_R^C \nu_R \quad (1.18)$$

We also have to add Dirac mass terms: the first Dirac mass term we mentioned on this section (Equation 1.19) and another one that comes from the charge-conjugate fields (Equation 1.20):

$$L = m_D \bar{\nu}_L \nu_R + m_D \bar{\nu}_R \nu_L \quad (1.19)$$

$$L = m_D \bar{\nu}_R^C \nu_L^C + m_D \bar{\nu}_L^C \nu_R^C \quad (1.20)$$

Since the hermitian conjugate of each equation is identical, we can write the most general mass term as:

$$L = \frac{1}{2} \left( m_L \bar{\nu}_L^C \nu_L + m_R \bar{\nu}_R^C \nu_R + m_D \bar{\nu}_R \nu_L + m_D \bar{\nu}_L^C \nu_R^C \right) \quad (1.21)$$

The former equation can be written as a matrix equation:

$$L_{mass} \propto \begin{pmatrix} \bar{\nu}_L^C & \bar{\nu}_R \end{pmatrix} \begin{pmatrix} m_L & m_D \\ m_D & m_R \end{pmatrix} \begin{pmatrix} \nu_L \\ \nu_R^C \end{pmatrix} \quad (1.22)$$

The Equation 1.22 expresses the Lagrangian in terms of the left and right chiral states. These states do not have a definite mass because the matrix is not diagonal. Thus, the left and right chiral states do not correspond to the physical particles (which have a definite mass). Instead the real particles are a superposition of the mass eigenstates. In order to find the mass eigenvalues we need to diagonalize the M



matrix (the one in the middle of the former equation). This calculation is explained in Appendix A. We find the mass eigenstates are given by the expression:

$$m_{1,2} = \frac{1}{2} \left[ (m_L + m_R) \pm \sqrt{(m_L - m_R)^2 + 4m_D^2} \right] \quad (1.23)$$

The fact that the SM does not allow a Majorana left-chiral mass term implies  $m_L = 0$ . Next, we are going to study the expression of the mass eigenstates  $m_1$  and  $m_2$ . When we choose  $m_R \gg m_D$ , we get for the mass eigenvalues:

$$m_1 = \frac{m_D^2}{m_R} \quad (1.24)$$

$$m_2 = m_R \left( 1 + \frac{m_D^2}{m_R^2} \right) \approx m_R \quad (1.25)$$

From both equations above we can deduce that if there a neutrino with mass  $m_2$  very large exists, then the other neutrino must have a small mass. The former fact is the reason why this mechanism is called “Seesaw”: the mass of each physical neutrino is controlled by the mass eigenvalues in a way such that when one neutrino is light the other is heavier. Now, the neutrino mass eigenstates are given by the following expresions:

$$\nu_1 \propto (\nu_L + \nu_L^C) - \frac{m_D}{m_R^2} (\nu_R + \nu_R^C) \quad (1.26)$$

$$\nu_2 \propto (\nu_R + \nu_R^C) + \frac{m_D}{m_R^2} (\nu_L + \nu_L^C) \quad (1.27)$$

The former equations show that  $\nu_1$  is mostly the left-handed light Majorana neutrino while  $\nu_2$  is the heavy sterile right-handed neutrino. This is the explanation that the Seesaw Mechanism gives to the fact that the neutrino is much lighter than the other fermions.

## Chapter 2

# CMS Detector

The CMS is one of the four experiments at the Large Hadron Collider (LHC), which is the largest and most powerful particle accelerator in the world. This accelerator collimates protons at very high energies of the order of 13 TeV, with the objective of studying the elementary particles of the universe. The LHC is composed by a ring of almost 27 km and by 4 detectors located at the different collision points of the ring. 2 of these detectors are general-purpose, they belong to the experiments CMS (Compact Muon Solenoid) and ATLAS (A Toroidal LHC Apparatus). Both experiments share the same goal of searching physics beyond the SM as: search and measurement of the Higgs boson, Supersymmetry searches, DM, detection of extra dimensions, among others. The difference between both experiments is that they use different technical solutions and the magnetic field is produced by a different system design. In the ATLAS detector the magnetic field is produced by a central toroid, two end toroids and a central solenoid, while the CMS detector is built around a solenoid magnet.

The CMS and ATLAS detectors have a cylindrical form in order to have the most uniform magnetic field possible, they are centered in the direction of the interacting beams and the collision point and have two “end-caps” to cover the forward regions. These detectors are composed by the same general components, from the inner part of the detector to the outer part, these are: a tracking system, an electromagnetic and a hadronic calorimeter and muon detectors. They also have magnets to

curve the path of the electric charged particles, so it can be determined if a particle has a positive or negative charge. The measurement of the curve can be used to calculate the momentum of the charged particle.

## 2.1 Accelerator and Storage Ring

## 2.2 Tracks Detector

Since every 25 ns almost 1000 particles are going to be produce in the center of the CMS detector, it is necessary to have a tracking system that covers this region. This tracking system must measure the momentum and vertices of the particles with a high precision. The tracking system is based on silicon detectors, with high granularity pixel systems at the smallest radii, and silicon-strip detectors at larger ones. The elements of the tracking system are fast taken measurements, tolerate high doses of radiation, are made of light material and resist the severe conditions imposed by low temperature. One of the major challenges for the inner detector parts is the control of aging effects because the damage produced by irradiation is severe. The silicon detectors are p-n junction diodes, so when a particle crosses the detector liberates electron-hole pairs, which move to the electrodes of the system. The tracking system in the CMS detector covers the range of  $|\eta| < 2.5$ , the region where most of the particles arrive.

The flux of particles arriving to the detector depends of the distance from the center of collision: as the flux crosses the detector the quantity of particles in it decrease. Thus, the resolution of the tracking system does not need to be so high in the intermediate and end caps of it. For this reason, in the first region of the tracking system (the closest to the interaction point), there are silicon pixel detectors with cell size of  $100 \times 150 \mu m^2$ . The innermost layer of pixels is located as near to the beam as it is practical, this is at a radius around 4.5 cm.

Due to the silicon pixels are expensive and have high power density, at the intermediate region of the tracking detector they are replaced by silicon microstrip systems. The former is also because at that region (at a radius between 20 and 55 cm) the flux of particles is low enough

to use this technology. These barrel cylinders and end-caps discs, as the silicon pixels ,cover the region of  $|\eta| < 2.5$  . The strip dimensions are or around  $11\text{cm} \times 100\mu\text{m}$ . These silicon microstrip are arranged in a special way to improve the resolution in the z axis.

In the outermost region of the tracking system (at a radius greater than 55 cm) the particle flux is low enough to use a larger-pitch silicon microstrips. The maximum size of these cells is  $25\text{cm} \times 80\mu\text{m}$ . There are 6 layers of this silicon microstrips moduls in the barrel and 9 end-caps discs that also cover the region given by  $|\eta| < 2.5$ .

## 2.3 Calorimetry

Surrounding the tracking system of the CMS detector is located the electromagnetic and hadronic calorimeter. The calorimeters measure the energy of the incoming particles, by absorbing it and transforming it into heat. The priority of the electromagnetic calorimeter is to measure precisely the energy of electrons and photons, to make measurements of their position and direction of movement. While, the priority of the hadronic calorimeter is to make precise measurements of the jets energy and to cover a larger area of  $|\eta| < 5$ , for the purpose of attributte all the  $\vec{E}_T^{miss}$  to the actual non-detected particles.

The electromagnetic and hadron calorimeter are made out of scintillation crystals. When a high energy particle goes through the detector, it collides with the nuclei of the material and generates a shower of particles. The product particles of this interaction excitate the atoms in the material by making the electrons in them go to a higher orbit. When each electron returns to the initial orbit, it emmits a photon.

Then, the ligh emmitted by the scintillator is measured by photodiodes

### 2.3.1 Electromagnetic Calorimeter

The electromagnetic calorimeter is an entirely active homogeneous calorimeter made of lead tungstate ( $\text{PbWO}_4$ ) crystal. It has 61,200 crystal in the central barrel part and 7,324 in each of the two end-caps. As a consequence of the use of high density crystals the calorimeter is fast, has

fine granularity and is radiation resistant. The lead tungstate crystal material was chosen for different reasons. First, it emits a short radiation length when a particle ionizes the material by crossing the crystal. Second, it has small Moliere radius, which is defined as the radius of the cylinder surrounding the 90% of the shower's energy deposition. The former leads to a compact calorimeter in size. Third, the lead tungstate crystal has short decay time constant, which allows the calorimeter to have a fast response. Lastly, it is resistant to high doses of radiation.

The electromagnetic calorimeter is located within the solenoid. The light emitted by the

### **2.3.2 Hadronic Calorimeter**

## **2.4 Muon Detector**

## **2.5 Triggers**

### **2.5.1 Triggers at the CMS**

## Chapter 3

# Important Concepts and Variable Definitions

### 3.1 Jets

A Jet can be defined as a high energy shower of stable particles that comes from fragmentation of quarks or gluons. The initial quarks and gluons in the process are known “initial partons”. Due to the initial partons are colour charged, they can not be isolated singularly (this phenomenon is called “colour confinement”. Since it is not possible for charged particles to be isolated they must go through a non-perturbative process that converts them into colour neutral particles. This process is called “hadronization” and there are different models to explain it. According to the string model, the confining nature of strong interaction increases the potential colour in a proportional way as the distance between the initial partons. When the distance reaches a certain critical value it is energetically favourable to produce a quark pair from the vacuum. Finally, by this process the initial colour charged particles are converted into bound colour-singlet hadronic states.

Besides jets may display a structure with properties that could indicate which were the initial partons interacting, they are hard to study individually when there is a numerous quantity of them in an event.

The former is because it is almost imposible to attach all particles in an event final state to a single initial parton. The reconstruction of jets depends of elements like the fragmentation process, detectors effects, among others. Thus, there exist algorithms which cluster some particles in a final state so that it is possible to determine properties as 4-momentum and jet shapes. The objeotive of this algorithms is to determine the inital interacting partons and approximate its directions and energies.

According to the reconstruction algorithms we can define a jet at three different levels. At partonic level a jet can be understood as a quark or a gluon. At hadronic level can be referred to the hadrons produced due to the hadronization process. Finally, at a detector level can be understood as a the tracks detected and the energy deposited in the calorimeters of the detector. The reconstruction algorithms that are going to be used for this analysis consist in enclose in cones the regions where there is a numerous detection of particles.

## 3.2 Cross Section and Luminosity

In High Energy Physics the cross section  $\sigma$  concept is the probability that a certain event of interest has to occur. This quantity is proportional to the energy of the event production. The unit used for cross sections is the bar ( $1 \text{ b} = 10^{-28} \text{ m}^2$ ). The number of a certain interaction in a fixed target experiment is proportional to its cross section, the particles flux, and the number of atoms per cubic meter in the target multiplied by the lenght. The inverse of the last quantity is called “target constant  $F$ ” and it has the dimesion of an area. Thus, it is possible to make an estimation of the number of interactions per second using:

$$\frac{N_{events}}{s} = \sigma \frac{N_{flux}/s}{F} = \sigma \times Luminosity \quad (3.1)$$

In the last identity we defined the concept of luminosity, which is a measure of sensitivity and depends on the energy and on the beam dynamics. The luminosity is a quantity that is used to describe the performance of a particle accelerator. It has units of the inverse of

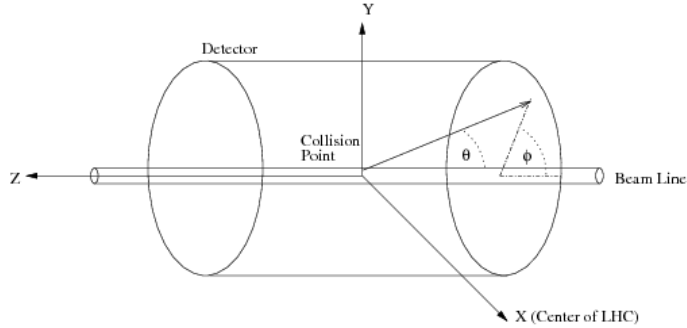
cross section, which is known as inverse barns  $fb^{-1}$  and it is equivalent to  $(1fb = 10^{-28}m^2)$ . In particle colliders the luminosity depends on different factors as the number of particles per bunch  $N_b$ , the number of bunches in each beam  $\kappa_b$ , the revolution frequency  $f$  at the storage ring and the beam radii  $\sigma$  of the bunches at the crossing point:

$$L = \frac{N_b^2 f \kappa_b}{4\pi\sigma^2} \quad (3.2)$$

### 3.3 Pseudorapidity

The variable Pseudorapidity is defined as a parametrization of the CMS detector coordinates. These coordinates are illustrated in the figure 3.3:

Figure 3.1: CMS detector coordinates



The origin of the CMS coordinates coincides with the point in which a collision occurs in the detector. The polar angle is described by the parameter  $\theta$  and it is measured with respect to the z axis. The azimuthal angle is denoted by  $\Phi$  and it is measured in the xy plane from the x axis. The Pseudorapidity is defined in terms of the polar angle as:

$$\eta \equiv -\ln(\tan(\theta/2)) \quad (3.3)$$

The motivation to define and use this variable is that while  $\Delta\theta$  is not a Lorentz invariant  $\Delta\eta$  is. Moreover, the quantity of particles in function on the variable  $\eta$  is approximately uniform in a cylindrical detector.



### 3.4 $p_T$ and $E_T^{\vec{miss}}$

The quantity  $p_T$  is the transversal momentum and it is the projection of the linear momentum onto the xy plane. This variable is used instead of the linear momentum because the initial beams are moving just in the z axis (the initial momentum in the xy plane is zero), so when a collision is produced the interesting effects occur in the transverse plane.

As it was already mentioned the momentum in the transverse plane is zero before the collision. Since the transverse momentum has to be conserved, after the collision it must be zero. We can write the total momentum as the sum of the particles that are detected (visible particles) and the ones that are not detected (invisible particles), the former can be expressed as:

$$0 = \sum_{i=1}^N P_T \vec{i} = \sum_{j=1}^M P_T \vec{j}^{visibles} + \sum_{k=M}^{N-M} P_T \vec{k}^{invisibles} \quad (3.4)$$

The former equation motivates the definition of a variable called “Missing transverse energy” ( $E_T^{\vec{miss}}$ ), which is defined as the sum of the transverse momentum of the invisible particles:

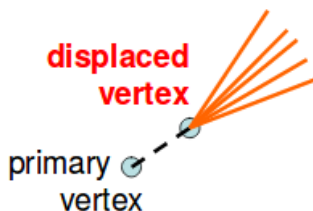
$$E_T^{\vec{miss}} \equiv \sum_{k=M}^{N-M} P_T \vec{k}^{invisibles} = - \sum_{j=1}^M P_T \vec{j}^{visibles} \quad (3.5)$$

### 3.5 Displaced Vertices and Impact Parameter

The vertex of a track is a variable of importance because it can be used to determine the position of the point of interaction and the momentum vector of the tracks emerging from the vertex. The vertex fit can also be used to check the association of tracks to a vertex, in other words, to determine if a track actually originates from a certain vertex. In order to determine the direction of the track connecting a primary and a secondary vertices we have to find the position of the secondary vertex.

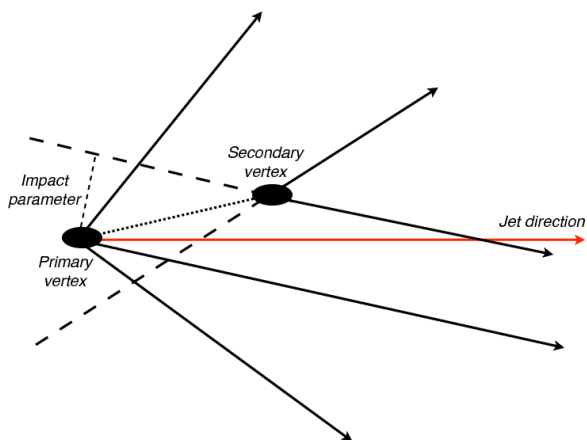
Some particles can pass through the detector without living tracks, when this particles decay, the particles produced can be detected and leave tracks on the detector. The point in which the product particles are detected is called a secondary vertex, and it is said that it is a displaced vertice. The former description is showed in the figure 3.5, where the path of the undetected particle is represent by a doted line:

Figure 3.2: Scheme of a displaced vertex



Now, the impact parameter is defined as the closest distance between the vertex and the points of the track. A visualization of this is showed in the figure 3.5. In this image the track is represented by the blue dotted line, and the impact parameter by the red line. It can be seen that the impact parameter line forms a right angle with the track. Using this characteristic it is possible to identify in a unique way the closest point of approach of the track to the vertex.

Figure 3.3: Scheme of the impact parameter variable



## Chapter 4

# Model and backgrounds

### 4.1 Signal of Interest

### 4.2 Backgrounds

#### 4.2.1 W + Jets Background

#### 4.2.2 Drell Yan + Jets Background

#### 4.2.3 $t\bar{t}$ Background

## Chapter 5

# Methodology

5.1 MadGraph

5.2 Pythia

5.3 Delphes

5.4 ROOT

## Chapter 6

# Analysis

## Chapter 7

# Event Selection Criteria

## Chapter 8

# Conclusions



# Appendix A

## Neutrinos and Seesaw Mechanism

First of all we are going to start by defining some fundamental concepts: helicity, quirkality and projection operators. The helicity of a particle is defined as the projection of its spin onto the direction of its motion. It is said that a particle is right-handed when its spin is in the same direction as its motion and it is said a particle is left-handed when its spin is opposite in the opposite direction of its motion. In the case of massless particles the concept of quirkality and helicity is equivalent. The quirkality for a Dirac fermion is defined through the operator  $\gamma^5$  with eigenvalues  $\pm 1$ . Thus a Dirac field can be projected into its left or right component by acting the operators  $P_R$  and  $P_L$  upon it. The right- and left-handed projection operators are defined as:

$$P_R = \frac{1 + \gamma^5}{2} \quad \text{and} \quad P_L = \frac{1 - \gamma^5}{2} \tag{A.1}$$

### A.0.1 Dirac Mass

In this Appendix we are going to perform with detail the calculations for neutrino physics which were mentioned in the State of the Art Chapter. We start here by studying the Dirac Mass, which is a term of the form:

$$m\bar{\psi}\psi = m(\overline{\psi_L + \psi_R})(\psi_L + \psi_R) = m(\overline{\psi_L}\psi_L + \overline{\psi_L}\psi_R + \overline{\psi_R}\psi_L + \overline{\psi_R}\psi_R) \quad (\text{A.2})$$

Lets study the term  $\overline{\psi_L}\psi_L$  and using  $P_R P_L = 0$ :

$$\overline{\psi_L}\psi_L = \overline{\psi}P_L^\dagger P_L\psi = \overline{\psi}P_R P_L\psi = 0 \quad (\text{A.3})$$

Using an analogous reasoning we can find  $\overline{\psi_R}\psi_R = 0$ , too. Finally, we obtain the expresion:

$$m\bar{\psi}\psi = m(\overline{\psi_L}\psi_R + \overline{\psi_R}\psi_L) \quad (\text{A.4})$$

### A.0.2 Majorana Mass

The expression we had for the Dirac Lagrangian was:

$$\begin{aligned} L &= \overline{\psi} (i\gamma^\mu \partial_\mu - m) \psi \\ &= (\overline{\psi_L} + \overline{\psi_R})(i\gamma^\mu \partial_\mu - m)(\psi_L + \psi_R) \\ &= i\overline{\psi_L}\gamma^\mu \partial_\mu \psi_L + i\overline{\psi_L}\gamma^\mu \partial_\mu \psi_R - m\overline{\psi_L}\psi_L - m\overline{\psi_L}\psi_R \\ &\quad + i\overline{\psi_R}\gamma^\mu \partial_\mu \psi_L + i\overline{\psi_R}\gamma^\mu \partial_\mu \psi_R - m\overline{\psi_R}\psi_L - m\overline{\psi_R}\psi_R \end{aligned} \quad (\text{A.5})$$

We already proved that  $\overline{\psi_L}\psi_L = \overline{\psi_R}\psi_R = 0$ . Now we are going to study the second term in the Equation A.5, which has a term of the form:

$$\begin{aligned} P_R \gamma^\mu &= \frac{1}{2}(1 + \gamma^5)\gamma^\mu = \frac{1}{2}(\gamma^\mu + \gamma^5\gamma^\mu) \\ &= \frac{1}{2}(\gamma^\mu - \gamma^\mu\gamma^5) \quad \text{Since } \{\gamma^5, \gamma^\mu\} = \gamma^5\gamma^\mu + \gamma^\mu\gamma^5 = 0 \\ &= \frac{1}{2}\gamma^\mu(1 - \gamma^5) = \gamma^\mu P_L \end{aligned} \quad (\text{A.6})$$

Using what we have found in the last expression, we get for the

second term:

$$\begin{aligned}
i\bar{\psi}_L\gamma^\mu\partial_\mu\psi_R &= i\bar{\psi}P_R\gamma^\mu\partial_\mu P_R\psi \\
&= i\bar{\psi}\gamma^\mu P_L\partial_\mu P_R\psi \\
&= i\bar{\psi}\gamma^\mu\partial_\mu P_L P_R\psi \quad \text{Since } P_L \text{ is a constant operator} \\
&= 0
\end{aligned} \tag{A.7}$$

Following a similar calculation we get:  $i\bar{\psi}_R\gamma^\mu\partial_\mu\psi_L = 0$ . Our next step is to find the two coupled Dirac equations using the Euler-Lagrange equation. We obtained for the Lagrangian:

$$L = i\bar{\psi}_R\gamma^\mu\partial_\mu\psi_R + i\bar{\psi}_L\gamma^\mu\partial_\mu\psi_L - m\bar{\psi}_R\psi_L - m\bar{\psi}_L\psi_R \tag{A.8}$$

Replacing in the Euler-Lagrange equation, we get for both states:

$$\begin{aligned}
\frac{\partial L}{\partial(\partial\bar{\psi}_R)} &= \frac{\partial L}{\partial\bar{\psi}_R} \rightarrow 0 = i\gamma^\mu\partial_\mu\psi_L - m\psi_R \\
\frac{\partial L}{\partial(\partial\bar{\psi}_L)} &= \frac{\partial L}{\partial\bar{\psi}_L} \rightarrow 0 = i\gamma^\mu\partial_\mu\psi_R - m\psi_L
\end{aligned} \tag{A.9}$$

Now, we are going to find an expression for  $\psi_R$  in terms of  $\psi_L$ . First, we take the hermitian conjugate of the bottom equation in A.9:

$$\begin{aligned}
i\gamma^\mu \partial_\mu \psi_R &= m\psi_L \\
(i\gamma^\mu \partial_\mu \psi_R)^\dagger &= m\psi_L^\dagger && \text{Taking the hermitian conjugate} \\
-i\partial_\mu \psi_R^\dagger \gamma^{\mu\dagger} &= m\psi_L^\dagger \\
-i\partial_\mu \psi_R^\dagger \gamma^{\mu\dagger} \gamma^0 &= m\psi_L^\dagger \gamma^0 && \text{Multiplying on the right by } \gamma^0 \\
-i\partial_\mu \psi_R^\dagger \gamma^0 \gamma^\mu &= m\psi_L^\dagger \gamma^0 && \text{Using } \gamma^{\mu\dagger} \gamma^0 = \gamma^0 \gamma^\mu \\
-i\partial_\mu \bar{\psi}_R \gamma^\mu &= m\bar{\psi}_L && \text{We have } \bar{\psi} = \psi^\dagger \gamma^0 \\
-i(\partial_\mu \bar{\psi}_R \gamma^\mu)^\dagger &= m\bar{\psi}_L^\dagger && \text{Taking the transpose} \\
-i\gamma^{\mu\dagger} \partial_\mu \bar{\psi}_R^\dagger &= m\bar{\psi}_L^\dagger \\
-i(-C^{-1} \gamma^\mu C) \partial_\mu \bar{\psi}_R^\dagger &= m\bar{\psi}_L^\dagger && \text{Using } \gamma^{\mu\dagger} = -C^{-1} \gamma^\mu C \\
i\gamma^\mu \partial_\mu C \bar{\psi}_R^\dagger &= mC \bar{\psi}_L^\dagger && \text{Multiplying on the left by } C
\end{aligned} \tag{A.10}$$

As we saw previously, for the lastest equation to have a similar structure as the top equation of A.9, the right-handed component of  $\psi$  must be:

$$\psi_R = C \bar{\psi}_L^\dagger \tag{A.11}$$

Now, we need to prove that  $C \bar{\psi}_L^\dagger$  is actually right-handed. To do this we apply the left-handed chiral projection operator  $P_L$  on this state and the result must be zero.

$$\begin{aligned}
P_L (C \bar{\psi}_L^\dagger) &= C P_L^\dagger \bar{\psi}_L^\dagger && \text{Property of C: } P_L C = C P_L^\dagger \\
&= C (\bar{\psi}_L P_L)^\dagger
\end{aligned} \tag{A.12}$$

Now, let us examine the term  $\bar{\psi}_L P_L$ :

$$\begin{aligned}
\bar{\psi}_L P_L &= (P_L \psi)^\dagger \gamma_0 P_L = \psi^\dagger P_L \gamma_0 P_L \\
&= \psi^\dagger \gamma^0 P_R P_L = 0
\end{aligned} \tag{A.13}$$

Hence  $C \bar{\psi}_L^\dagger$  is in fact a right-handed quiral state.

## Appendix B

# Charge Conjugation Operator